Sensors & Diagnostics

PAPER

View Article Online
View Journal | View Issue

Cite this: *Sens. Diagn.*, 2023, **2**, 1311

A water soluble fluorescent probe for selective and sensitive detection of picric acid – a nitroexplosive†

Porchezhiyan Vadivel, ‡ Kalaivani Dayanidhi ‡ and Noorjahan Sheik Eusuff *

A novel water soluble material was synthesized and employed as a sensing probe towards a common nitro-aromatic explosive, namely, picric acid (2,4,6-trinitrophenol). The probe was prepared in a four step process, including extraction of saponin, oxidation of saponin into sapal, intrusion of pyrene and dip coating on a chitosan film. The oxidation of saponin into sapal was determined by DNPH assay. The saponin (SAP), oxidized saponin (SAPAL) and SAPAL-PY were well characterized by UV–vis, fluorescence, FT-IR, AFM, SEM and NMR spectroscopy methods. The sensing studies were carried out with SAPAL-PY, which has shown a highly selective "turn off" sensing behavior towards picric acid with a good sensitivity and detection limit of 5×10^{-10} ML^{-1} and was selective over other nitroaromatics. Also, the SAPAL-PY dip-coated chitosan film showed a very effective detection of picric acid within the concentration range of 0 to 10^{-9} M. The simplicity, selectivity and sensitivity of the proposed probe make it a potential sensor to detect nitroexplosives. Furthermore, the detection process of picric acid was reversible and repeatable for five cycles.

Received 18th July 2023,
Accepted 17th August 2023

DOI: 10.1039/d3sd00184a

rsc.li/sensors

1. Introduction

The detection of nitroaromatic compounds (NAC), habitually used as explosives, is pivotal in order to avert terrorist activities as well as to curb the detrimental consequences on health caused by its contamination.[1,2] The nitro-aromatic phenolic compound 2,4,6-trinitrophenol (TNP), commonly known as picric acid (PA), is one of the potent pollutants and a toxic explosive widely used in world wars due to it high energy content compared to that of TNT.[3,4] Other applications of PA include in dye synthesis, rocket fuel, fireworks, colored glass, *etc.*, and its release in the environment causes contamination in the air, water and soil.[5] In humans, PA exposure can lead to respiratory problems, liver damage, headaches, abnormal production of methemoglobin, skin diseases, *etc.*[6] Their explosive and harmful nature means the summit is sensitive and selective detection techniques. Hence the detection of PA is crucial.[7]

So far, various detection methods have been applied for sensing PA, which include chromatographic techniques,[8–10] ion mobility spectrometry,[11] mass spectrometry,[12] surface enhanced Raman spectroscopy,[13] capillary electrophoresis,[14] amperometry,[15] energy-dispersive X-ray analysis,[16] membrane electrode methods, electrochemistry analysis,[17,18] and so on.[19] No matter how, most of these techniques or methods are limited in their use on real samples as well as on-site testing due to a few drawbacks, like low sensitivity, requirement of sophisticated equipment, and sample pre-treatment. On the contrary, fluorescence techniques have grabbed attention for sensing PA due to their facile sample preparation, high sensitivity and selectivity, and low cost.[6,20,21] Owing to the advantages of fluorescence techniques, numerous probes have been developed thus far for the turn-off detection of PA and, to list a few, metal organic frameworks, polymers, quantum dots, nanomaterials *etc.*[22–25]

Saponin based biomaterials are meager in number owing to the hemolytic nature and chemical inertness associated with it. Generally, natural surfactants like saponin are used as either emulsifiers[26] or adjuvant in vaccines.[27] Predominantly physical interactions are more prevalent than chemical interactions in natural surfactants. This is due to the presence of inert functionalities. The saponins are secondary metabolites present in leaves, fruits and barks of certain plants. They can be extracted from natural sources, like soapnut (*Sapindus mukorossi*), fenugreek seeds, legumes, tomato seeds, *etc.*[28] They exhibit many biological activities, like antimicrobial, anti-diabetic and anti-cancer ones.[29] In

PG & Research Department of Chemistry, Guru Nanak College (Autonomous), Affiliated to University of Madras, Velachery, Chennai, Tamil Nadu, India. E-mail: senoorjahan@gmail.com, noorjahan.se@gurunanakcollege.edu.in

† Electronic supplementary information (ESI) available: Optimization conditions for SAP oxidation, calibration graph of DNPH, calibration graph of periodate. See DOI: https://doi.org/10.1039/d3sd00184a

‡ Porchezhiyan Vadivel and Kalaivani Dayanidhi contributed equally to this manuscript.

most of the reported literature, the sensor solution is used in an organic solvent or in a mixture of water and organic solvent. Hence, in this study, a naturally and abundantly available soapberry pericarp of *Sapindus mukorosii* was made use of in the preparation of a water soluble probe.

In view of the above discussion, herein we have designed a probe by utilizing saponin (SAP) extracted from *Sapindus mukorosii*, commonly known as soapnut, and funtionalized it for the first time into SAPAL (aldehyde). The pyrene fluorophore was chosen as it could be excited at a wavelength of around 350–420 nm, which brings a coherence and low cost for the instrumentation. Also, the pyrene moiety has a very good chemical stability and prolonged fluorescence time.[30] Thus, this designed probe (SAPAL-PY) consisted of pyrene fluorophores as the sensing unit and cross-linkable saponin aldehyde that can be immobilized on chitosan or other polymeric films for the flexible and recyclable detection of picric acid.

2. Materials and methods

2.1. Materials

Soap nut (*Sapindus mukorossi*) was purchased from grocery stores in Chennai, India. Other chemicals, like sodium periodate, 2,4-dinitrophenylhydrazine (DNPH), ammonium sulfate, ethyl acetate and isopropyl alcohol, were purchased from Merck, India. Double distilled water was used throughout the studies.

Caution! The nitroaromatic compounds (PA) are powerful explosives and therefore should be handled with caution and also in very small quantities. They must be stored in bottles with about 50% water for safety reasons.

2.2. Isolation of saponin from the powdered pericarp of *S. mukorossi*

A suspensions of 75 g of the powdered *S. mukorossi* in double distilled water was heated on an oil bath for 6–8 h. The solution was filtered using a strainer; the filtrate was kept in a water bath for 2 h at 60 °C and then treated with solid ammonium sulfate with vigorous stirring until a gelatinous mass floated on the surface. The gelatinous mass was filtered off and the process was repeated. The collected gelatinous mass was dissolved in saturated ammonium sulfate and extracted with ethyl acetate. The ethyl acetate layer was separated and evaporated to dryness, to yield saponin as a creamy white solid weighing 7 g.

2.3. Periodate oxidation of saponin

Sodium periodate was added to 100 mL of 1% (w/v) aqueous saponin solution and stirred for a particular period of time and temperature. The vials were wrapped with aluminum foil so as to protect it from light. After completion of the reaction, the reaction mixture was poured into a beaker containing isopropyl alcohol (IPA) and then stirred for an hour to get a white solid of SAPAL, which was stored in an airtight container at room temperature. Optimization of the amount of sodium periodate, reaction time and temperature required to yield a higher aldehyde content was carried out by varying the amount of sodium periodate from 0.2 to 1.8 g, a time period of 1–6 h and a temperature a 35–55 °C. The optimization conditions are given in Table S1 (ESI†).

2.4. Preparation of the DNPH solution

About 0.01 g of DNPH solution was dissolved in 1 mL of concentrated sulfuric acid and stirred to complete dissolution, followed by the addition of 10 mL of ethanol. The resulting solution was diluted to 100 mL with double distilled water to prepare a 0.01 wt% of DNPH solution.

2.4.1. Determination of the aldehyde content of SAPAL through a DNPH assay. The aldehyde of SAPAL and the $-NH_2$ of DNPH reacted instantaneously to precipitate the hydrazone. The DNPH assay was carried out by adding 6 mL of freshly prepared 0.01% DNPH solution to 25 μL of various concentrations of SAPAL and made up to a final volume of 15 mL with double distilled water. After allowing the reaction mixture to stand for 30 min, it was centrifuged at 10 000 rpm for 10 min, the pellet (hydrazone) was discarded, while the supernatant with unreacted DNPH was collected and its absorbance measured in UV spectroscopy at 345 nm. One equivalent of DNPH reacts with one equivalent of aldehyde. So the amount of DNPH reacted will be equal to the amount of aldehyde generated. The formation of hydrazone by the reaction of SAPAL and DNPH is shown in Fig. 1, and the reaction is displayed in Fig. 2. The calibration graph of DNPH with glutaraldehyde (GA) as the control is given in Fig. S1 (ESI†). The aldehyde content can be determined by calculating the reacted DNPH concentration using the following expression (1)

$$\text{Aldehyde concentration (mmol per gram)} = \frac{\text{Reacted DNPH}/198.14}{2.5 \times 10^{-4}} \quad (1)$$

where 198.14 is the molecular weight of DNPH and 2.5×10^{-4} is the dilution factor.

2.4.2. Determination of the degree of oxidation of SAP. The concentration of periodate taken initially and that consumed after time intervals can be determined with the help of UV-vis spectroscopy by measuring the absorbance at 290

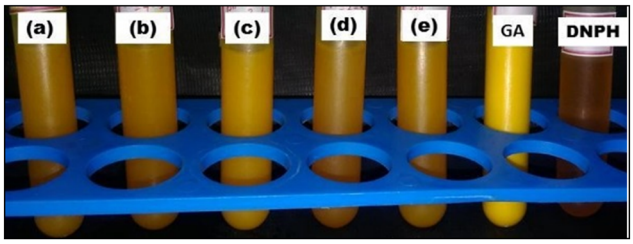

Fig. 1 (a–e) DNPH hydrazine of SAPAL of varying aldehyde content, GA – glutaraldehyde, DNPH – 2,4-dinitrophenyl hydrazine.

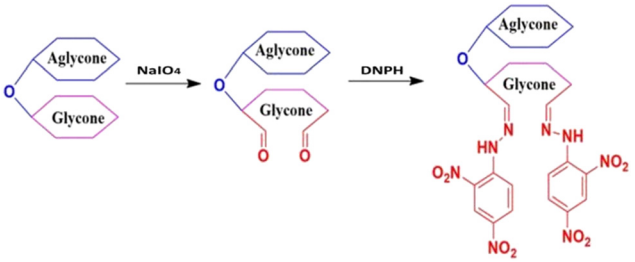

Fig. 2 Oxidation of saponin followed by reaction with DNPH.

nm, and the amount of unreacted periodate was calculated from the calibration graph (Fig. S2†). The degree of oxidation can be given by using the following expression (2).

$$\text{Degree of Oxidation (\%)} = \left[\frac{\text{CPA}_c}{\text{CPA}_i}\right] \times 100 \quad (2)$$

where CPA_i and CPA_c are the initial and unreacted periodate concentration, respectively, at time intervals.

2.4.3. Preparation of the SAPAL-PY fluorescent probe for the detection of PA. The fabrication of the SAPAL-PY fluorescent probe is as follows: the pyrene chromophore solution was added dropwise into the SAPAL solution and the mixture was sonicated for 5–10 min in an ultrasonic bath. The pyrene moiety was incorporated into SAPAL and the fabricated SAPAL-PY probe was evaluated for sensing PA. For this, PA standard solutions were prepared in different concentrations from 10^{-2} to 10^{-12} M and about 50 μL of the prepared solutions were added to 500 μL of SAPAL-PY and subjected to a fluorescence analysis. Also, for the selectivity of sensing, 50 μL of several other analytes were added to 500 μL of SAPAL-PY and the procedure was repeated.

3. Results and discussion

3.1. Optimization of the reaction parameters on the oxidation of SAP

On varying one of the parameters, like the periodate content, reaction time and temperature, and keeping the other two parameters constant, the aldehyde content measured showed a common trend. The aldehyde content was maximum for 1.2 g of sodium periodate and 4 h of reaction time (Fig. 3(a and b)). At first the aldehyde content increased slowly, reached a maximum and then gradually decreased. This decrease may be due to the degradation of SAP with an increase in sodium periodate content and reaction time, due to an extensive glycosidic oxidative cleavage. Similar results have been reported for the periodate oxidation of cellulose by Liu *et al.*[31] It was predicted that the degradation of cellulose can be prevented if a low concentration of periodate for a long reaction time or a high concentration of periodate for a short reaction time was employed. So, it is obvious that saponin being a small molecule will get degraded easily at a

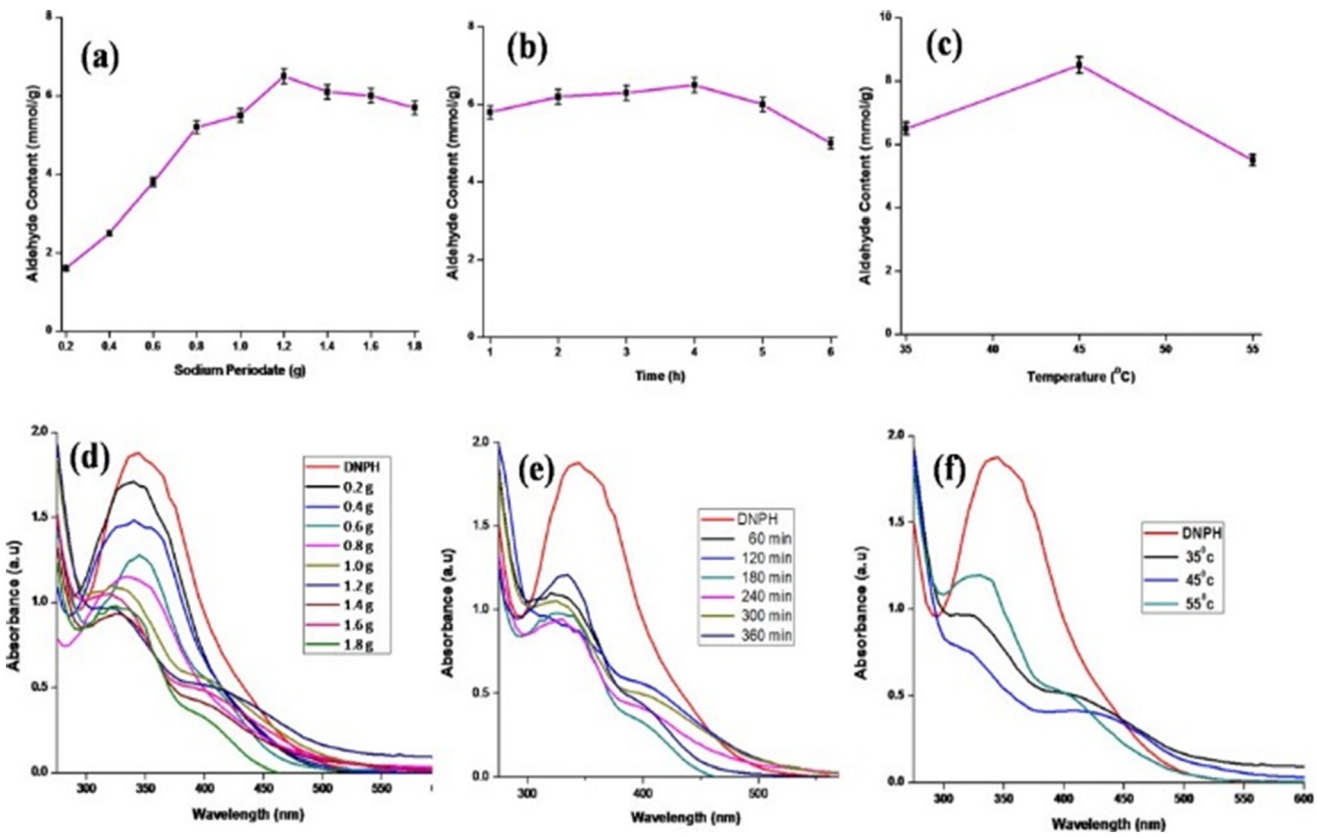

Fig. 3 Optimization of the amount of periodate (a and d), time (b and e) and temperature (c and f).

higher periodate content, whereas cellulose, being a polymer, could not withstand a higher amount of periodate.

The effect of temperature on aldehyde content is represented in Fig. 3c, where it can be seen that the aldehyde content increases from 35 °C to 45 °C and then decreases at 55 °C. The main reason being that at higher temperatures the sodium periodate starts decomposing with iodine evolution.[32] Hence, the aldehyde content was a maximum at 45 °C with 8.5 mmol g^{-1}, as given in Fig. 3c. Therefore, the optimum parameters to get a higher aldehyde content are as follows: amount of periodate – 1.2 g; time – 4 h; and temperature – 45 °C. The degree of oxidation calculated using the periodate absorbance at 290 nm for the optimized conditions was 86%. Fig. 3(d–f) represents the UV-spectrum obtained with the optimization of various parameters.

3.2. Fluorescence study

Saponin extracted from *S. mukorossi* exhibits a natural fluorescence emission in the range of 450–460 nm.[33] When the fluorescence emissions of SAP and SAPAL were measured, a strong fluorescence emission with a maxima at 460 nm was obtained. But the fluorescence intensity of SAPAL was reduced, which may be due to the structural modifications that occurred during the functionalization of SAP. Fig. 4 shows the fluorescence emission spectra of SAP and SAPAL.

3.3. IR spectroscopy analysis

The FTIR spectra of SAP and SAPAL are given in Fig. 5. The FTIR spectrum of SAP has a broad, intense band in the range between 3700 and 3200 cm^{-1} which can be attributed to the presence of –OH groups of the glycone moiety and the peak at 2931 cm^{-1} can be attributed to the aliphatic –C–H stretching vibrations of both the glycone and aglycone moieties. The narrow band in the region 1725–1625 cm^{-1} corresponds to the carbonyl group of aglycone, probably due

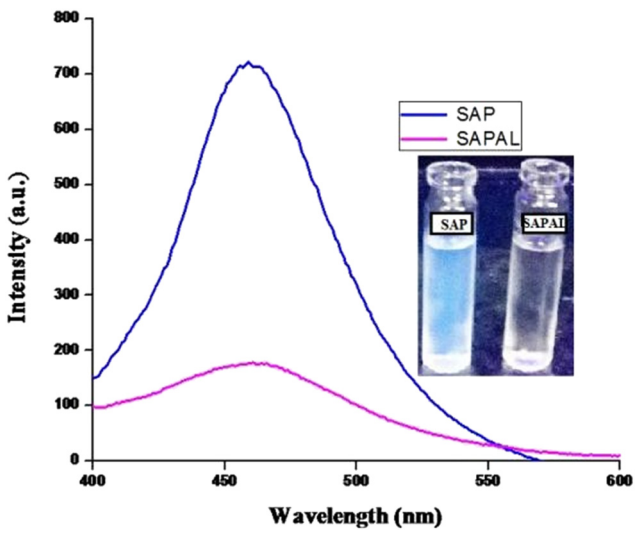

Fig. 4 Fluorescence emission spectra of SAP and SAPAL.

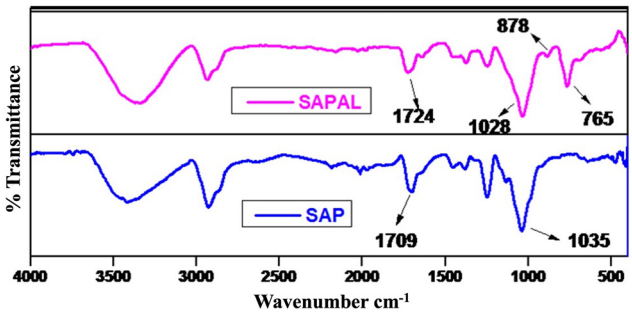

Fig. 5 FTIR spectra of SAP and SAPAL.

to the presence of an acid group.[34] The glycone (sugar) and aglycone (non-sugar) components are linked through an ether linkage (–C–O), evidenced by the peak centered at 1035 cm^{-1}. The presence of a carbonyl group in saponin suggests that it is a oleanane-type triterpenoid saponin.[35] In addition to the above mentioned peaks, the FTIR spectrum of SAPAL contains strong evidence for the presence of aldehyde groups, indicated from the shifting of the carbonyl peak from 1709 cm^{-1} (in saponin) to 1724 cm^{-1}. The –CHO groups get converted into hemiacetal, which is evident from a new peak appearing in the region 900–875 cm^{-1}, as reported earlier involving the oxidation of the polysaccharide – xylan.[36]

3.4. AFM analysis

The AFM images of SAP, SAPAL and SAPAL-PY are given in Fig. 6. The topography of SAP, SAPAL and SAPAL-PY was characterized by tapping mode AFM. From the AFM images (2D and 3D), it can be inferred that SAP, SAPAL and SAPAL-PY form micelles with well-defined boundaries with the average length of the micelle being 30.6 nm, 11.3 nm and 44.4 nm, respectively. The decrease in micelle size of the functionalized saponin suggests that there was a decrease in the actual molecular size and this may be due to the oxidative cleavage that has taken place during the oxidation of SAP. The SAPAL-PY showed a very clear micelle structure.

3.5. DLS analysis

The DLS measurements of SAP, SAPAL and SAPAL-PY are given in Fig. 7(a–c). The size distribution is measured using % intensity, which is a reliable method for measuring particle size. Table 2 gives the corresponding *Z*-average size, PDI values, % intensity and zeta potential of the particles. The *Z*-average sizes of particles measured using DLS technique were larger than those determined using AFM and FESEM. This deviation arises for polydispersed samples or mixtures of differently sized samples.[37] Even though the values are on the higher side, we could correlate and get useful information regarding the size of the particles. The average size of SAP was found to be greater than that of SAPAL. This confirms that SAPAL has a smaller particle size, as these may result due to the oxidative cleavage of SAP, and are in good agreement with the results (Fig. 8) obtained from FESEM.

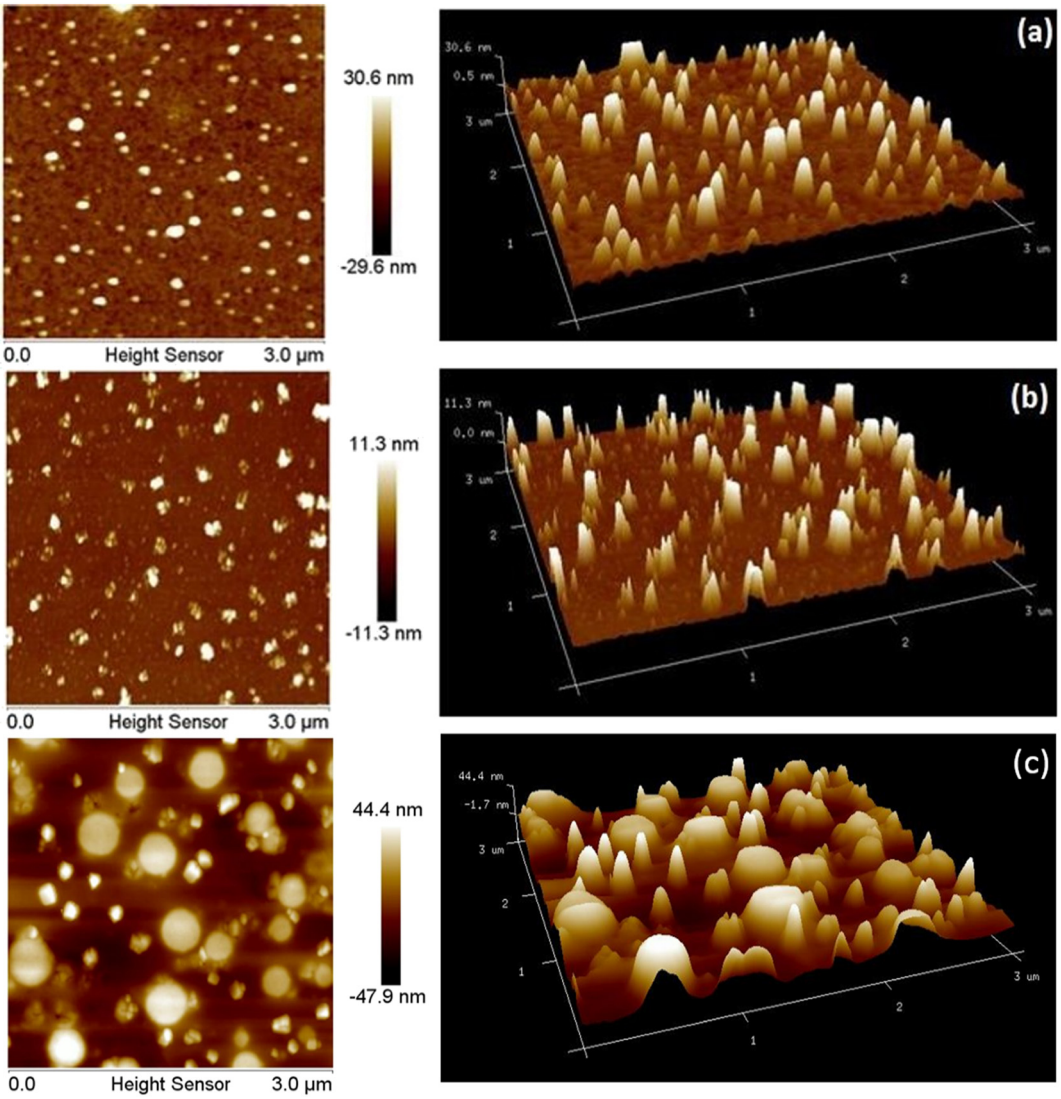

Fig. 6 AFM images of (a) SAP, (b) SAPAL and (c) SAPAL-PY.

The zeta potential is an important tool for understanding the state of the particle surface and predicting the long-term stability of the particle.[38] Zeta potential values of SAP, SAPAL and SAPAL-PY are given in Table 2. SAP exhibits a zeta potential of −34.4 mV, which suggests the accumulation of charges due to non-bonding electrons of the oxygen atom (–OH) and thereby achieving stabilization of the micelles. Similar zeta potential values have been reported by Behera *et al.* during the green synthesis and characterization of cuprous oxide nanoparticles in the presence of a bio-surfactant, wherein the saponin capped cuprous oxide nanoparticles exhibited −12 mV and the cuprous oxide without a surfactant exhibited only −6 mV. It is notable that SAPAL-PY exhibited −31.3 mV. The increase in zeta potential was mainly due to the presence of saponin.[39] SAPAL, the product obtained by the oxidative cleavage of the glycone moiety of saponin exhibited −29.2 mV, which predicts a lower number of –OH groups in it and hence fewer non-bonding electrons accumulate.

3.6. SEM analysis

The surface morphology of SAP, SAPAL and SAPAL-PY are given by FESEM photographs represented in Fig. 8. The FESEM images reveal the micelle structures of SAP, and SAPAL are spherical and bead like structures having a diameter 70–100 nm and 40–50 nm, respectively. The AFM and FESEM results have confirmed that SAPAL-PY could form well-defined micelles.

3.7. NMR analysis

Due to the decrease in aldehyde content with the formation of hemiacetal, identifying the –CHO group with the help of liquid NMR was difficult[40] and hence solid state NMR analysis was carried out. Fig. 9(a and b) represents the solid state NMR of SAP and SAPAL. The NMR spectrum of SAPAL clearly shows the presence of –CHO at 8.9 ppm, whereas in the SAP spectrum only the –OH peak at 6.1 ppm was recorded. The presence of –CHO was further confirmed by

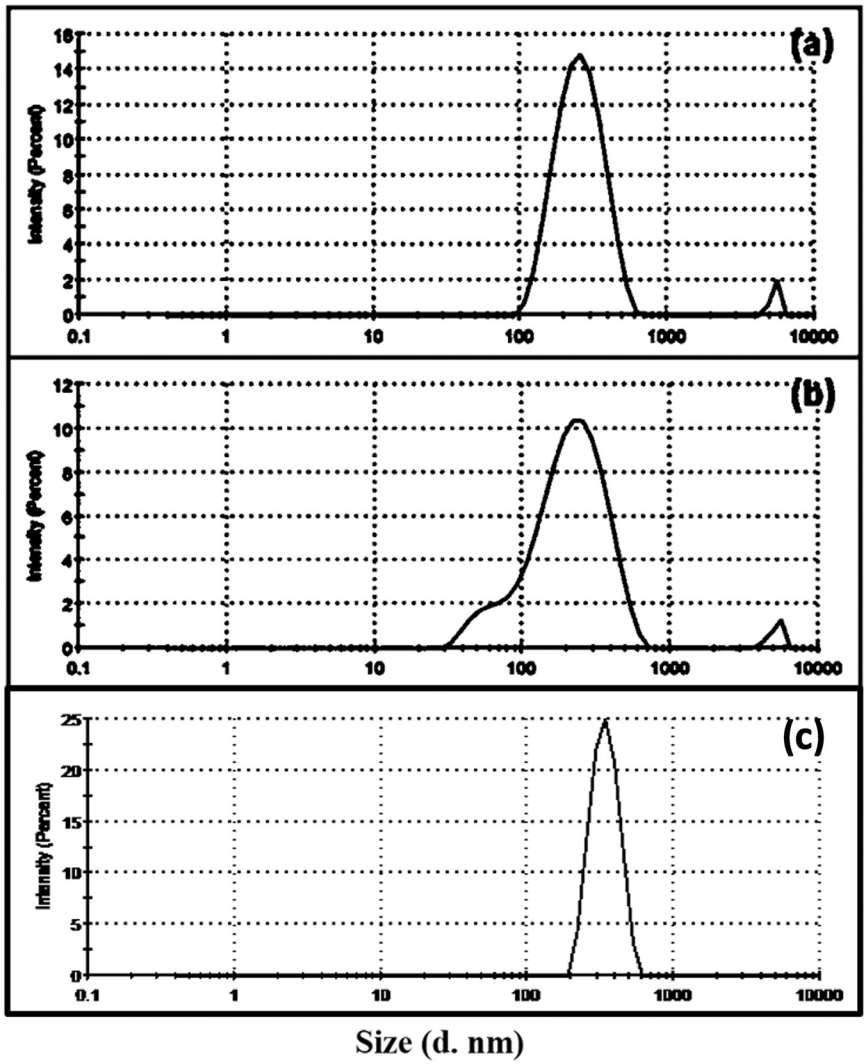

Fig. 7 DLS spectra of the intensity distribution of (a) SAP, (b) SAPAL and (c) SAPAL-PY.

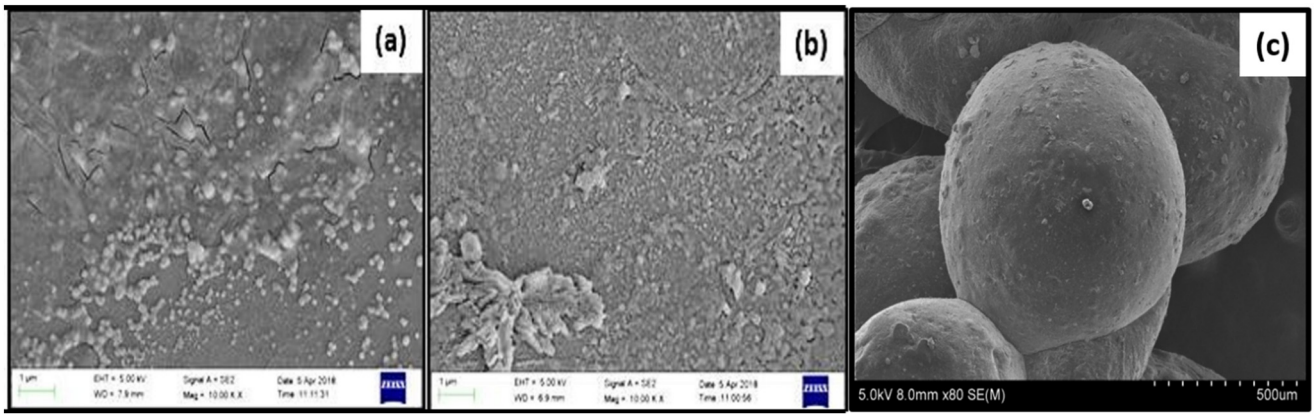

Fig. 8 FESEM images of (a) SAP, (b) SAPAL and (c) SAPAL-PY.

forming hydrazone with 2,4-dinitrophenylhydrazine (DNPH). The ^{1}H NMR and ^{13}C NMR of hydrazone are given in Fig. 9(c and d).

During the hydrazone formation, –CHO of SAPAL and $–NH_2$ of DNPH would react to form –CH═N, the imine bond, which is represented by the ^{1}H NMR peak (Fig. 9(c)) at 9.1

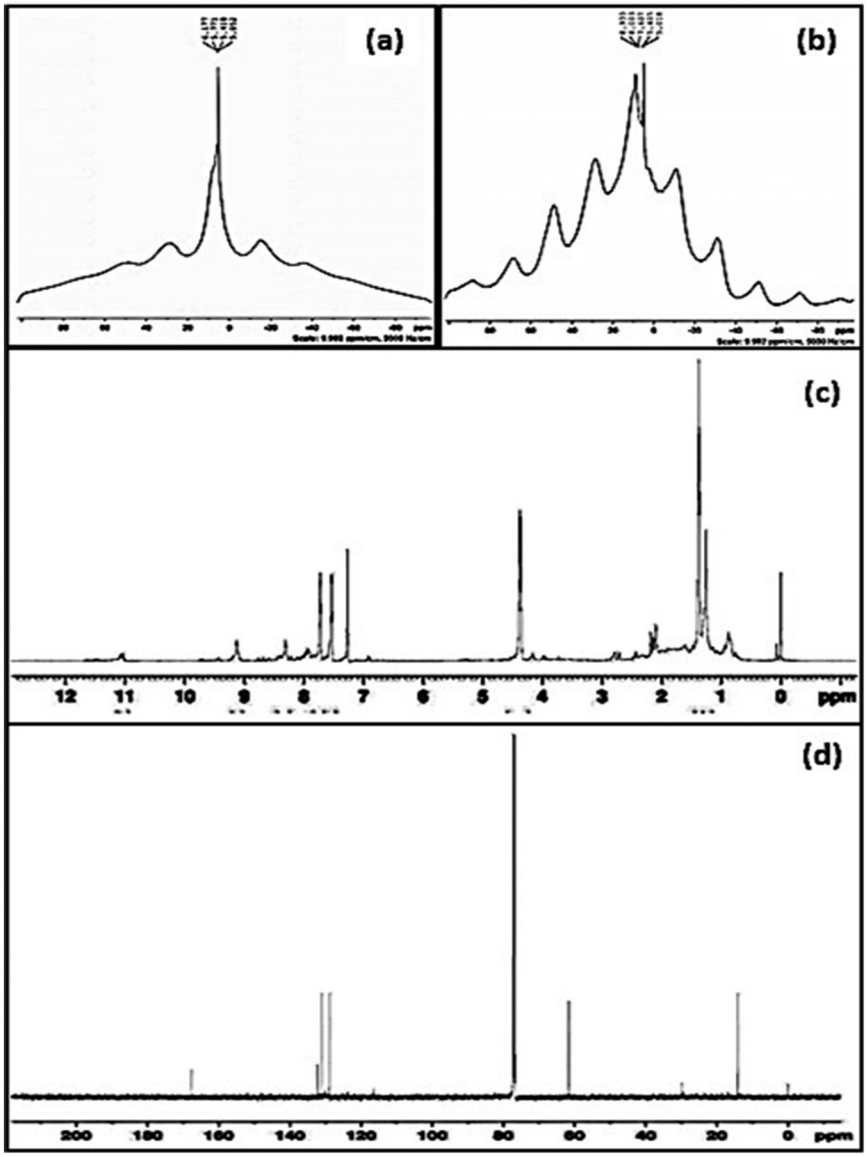

Fig. 9 (a) Solid state ^{1}H NMR of SAP, (b) solid state ^{1}H NMR of SAPAL, (c) ^{1}H NMR of the hydrazone of SAPAL with DNPH, and (d) ^{13}C NMR of the hydrazone of SAPAL with DNPH.

ppm and the presence of the –NH group of DNPH is confirmed by the small, broad peak at 11.1 ppm.[41] The aromatic hydrogens of DNPH and the aliphatic hydrogens are confirmed by the peaks in the ranges 7.3–8.4 ppm and 0.8–2.7 ppm, respectively. The formation of hemiacetal can be confirmed by the peak at 4.4 ppm.[42] The ^{13}C NMR spectrum also confirms the presence of –CH═N at 169 ppm and signals due to the aromatic carbons can be observed in the range 128–134 ppm. The aliphatic methylene carbons of SAPAL resonate at 17 ppm.[43]

3.8. Sensing studies

PA-sensing studies were carried out in aqueous media and a striking fluorescence quenching was observed on the gradual addition of PA. This turn-off fluorescence detection of PA can be observed by the naked eye under a UV lamp irradiated at 365 nm, as shown in the inset in Fig. 11. In an aqueous solution, PA dissociates to H+ and picrate immediately and interacts with SAPAL-PY, thereby quenching the fluorescence emission. Also, as shown in Fig. 10b, SAPAL-PY exhibited the highest selectivity for PA compared to that of other nitroaromatics with a phenolic group (NP and DNP-, which also showed a slight fluorescence quenching). This could be attributed to the electrostatic interaction between picrate and SAPAL-PY as PA is the strongest acid with pKa = 0.38.[44]

In order to evaluate the selectivity of SAPAL-PY towards PA detection, the fluorescence spectra of SAPAL-PY on the addition of PA and several other analytes, like 4-nitrophenol, 2,4-dinitrophenol, oxalic acid, citric acid, benzoic acid, and

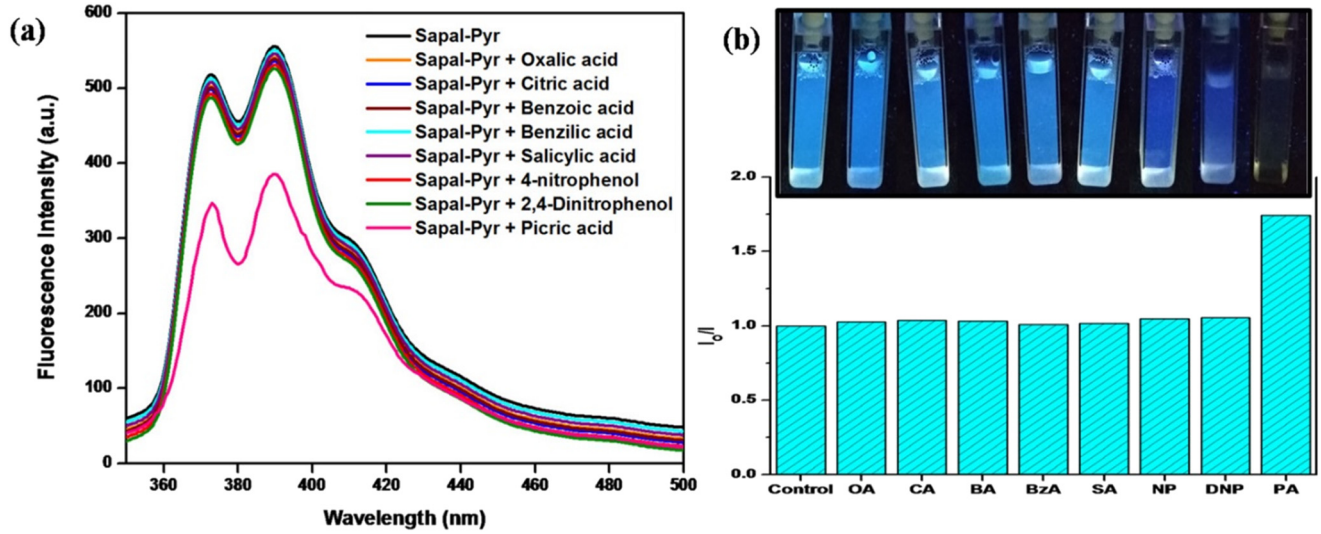

Fig. 10 (a) Fluorescence spectra. (b) Relative intensity of SAPAL-PY in the presence of PA and other analytes.

benzilic acid, were recorded under similar conditions. All the results are depicted in Fig. 10, from which it is obvious that fluorescence quenching occurred only in the presence of PA. Also, from Fig. 10b, it could be inferred that the relative intensity ratio (I_0/I) values are too high for PA than for the other analytes. All these results shows that SAPAL-PY has an excellent specificity in sensing PA.

Even though the water soluble sensors are simple and rapid for a real-time detection of nitro aromatic compounds in environmental samples, from the perspective of practical applications, film sensors are advantageous due to certain factors like reversibility, re-usability, and ease in the fabrication of lab-on-a-chip devices.[45] For this, chitosan was chosen as a suitable material for film fabrication, on account of the simple fabrication methods, like solution casting, dip coating, *etc.* As a result of its pH dependent solubility and its compatibility with the near-neutral physiological conditions, it is possible to design stable films on diverse surfaces under neutral as well as basic pH conditions. In addition, chitosan films can be easily functionalized with other substances, namely, polymers, nanomaterials, biomolecules, dye moieties, *etc.*[46]

Evoked by the favorable results of this probe in solution, we ventured to fabricate SAPAL-PY incorporated chitosan films for the convenient detection and monitoring of PA. For this, the chitosan films were immersed in a SAPAL-PY solution for a few minutes, then dried. Fig. 12 shows the sensing responses of the SAPAL-PY chitosan film to PA at various concentrations which were visualized under the irradiation of an UV chamber (365 nm) and visible light. Thus, this detection method would be beneficial for the field testing of PA with good selectivity and sensitivity.

One of the effective approaches in chemical sensing and surface studies is the fluorescence quenching method. In general, the quenching process can be analyzed by the Stern–Volmer eqn (3).

$$\frac{I_0}{I} = 1 + K_{SV}[PA] \quad (3)$$

where I_0 and I are the fluorescence intensities of SAPAL-PY in the absence and presence of picric acid [PA]. The slope of the plots gives the Stern–Volmer quenching constant (K_{SV}) (Fig. S3†). It is seen from the Stern–Volmer plot (Fig. S3†) that the change of I_0/I with respect to the PA concentration is linear at the lower concentrations of PA and results in a quenching constant (K_{SV}) of 1.4×10^{-6} M^{-1}, which suggests the quenching of the fluorescence of SAPAL-PY upon the addition of PA. This is ascribed to static quenching through the formation of a nonfluorescent ground-state complex, which after excitation returns to the

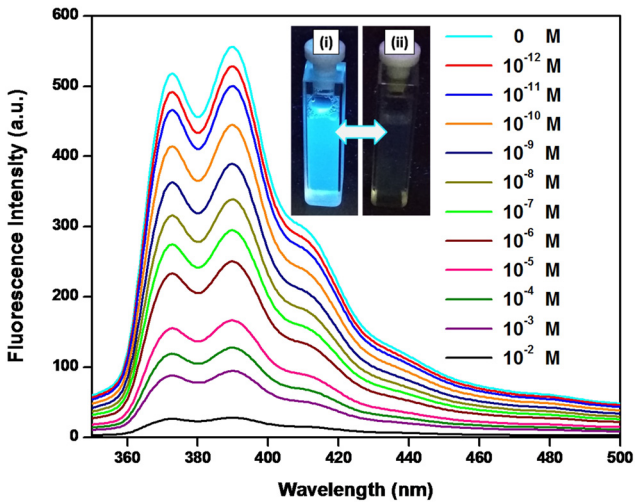

Fig. 11 Fluorescence spectra of SAPAL-PY in the presence of different concentrations of picric acid (inset: (i) SAPAL-PY and (ii) SAPAL-PY with picric acid).

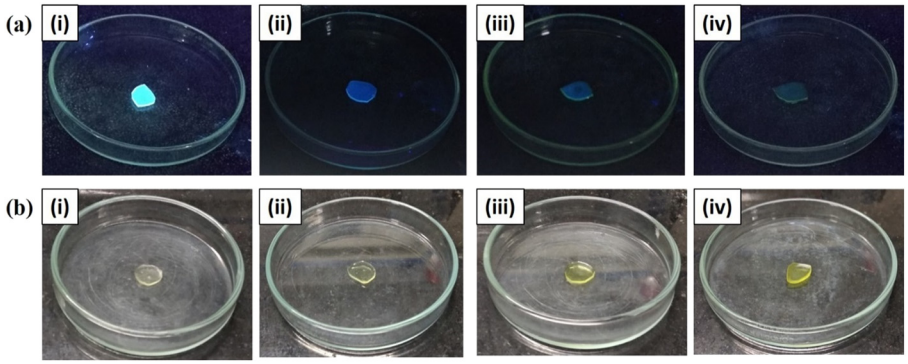

Fig. 12 Sensing response photographs of SAPAL-PY incorporated chitosan films with PA at concentrations of (i) 0 M, (ii) 10^{-2} M, (iii) 10^{-5} M, (iv) 10^{-9} M under. UV lamp-365 nm and (b) visible light.

ground state without the emission of light. However, a steep curve at a higher concentration of PA is possibly due to dynamic quenching.

Also, the quenching efficiency was calculated using eqn (4) as follows,

$$\eta = \frac{I_0 - I}{I_0} \times 100\% \quad (4)$$

The quenching efficiency plot is depicted in Fig. S4.† According to a method mentioned in the literature,[26] the equation used for calculating the detection limit is as follows:

$$\mathrm{DL} = C_\mathrm{L} \times C_\mathrm{T} \quad (5)$$

where DL is the detection limit, C_L is the concentration of SAPAL-PY, and C_T is the concentration of PA at which a sharp change in the peak is observed. From Fig. S5,† the limit of detection was found to be 5×10^{-10} ML^{-1}, indicating that SAPAL-PY could be a promising sensor for PA detection in water.

The reusability and reversibility of sensing process of the SAPAL-PY incorporated chitosan film was affirmed by fluorescence spectroscopy analysis. After every cycle of PA sensing, the recovery of the film was achieved by washing the film in distilled water. The film was reused after washing with water for sensing PA. The process was repeated five times and the recyclable efficiency is depicted in Fig. 13. Also, a cyclic graph on the reversibility of sensing film to PA is depicted in Fig. S6.† Moreover, a comparative study of our work with other reported literature is tabulated in Table 1, which shows that the fluorescent probe prepared in this study is more cost effective with a good detection limit. Thus, this stable fluorescent probe could be used for sensing PA in real-life applications.

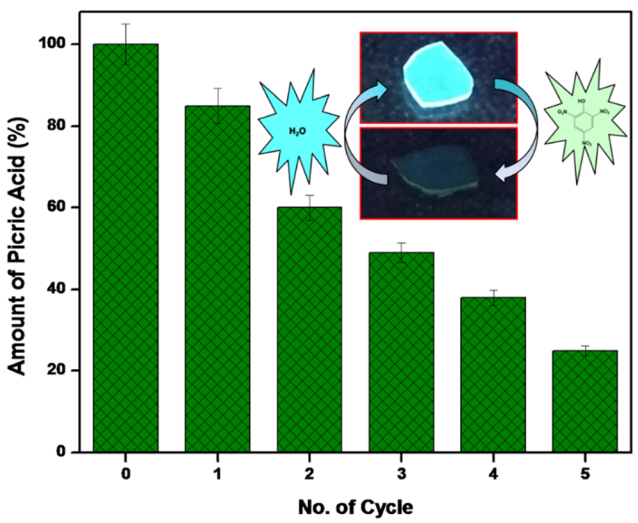

Fig. 13 Reversible and repeatable detection of picric acid (10^{-5} M) up to five cycles.

Table 2 Data from DLS measurements

Particles	*Z*-Average (nm)	PDI	% Intensity	Zeta potential (mV)
SAP	272.1	0.331	97.4	−34.4
SAPAL	177.2	0.368	97.7	−29.2
SAPAL-PY	496.2	0.416	98.4	−31.3

Table 1 Comparison of different fluorescent probes for the detection of picric acid

Fluorescent probe	Sensing medium	Sensing method	LOD	Ref.
Pyrene moieties on a glass surface with benzene	Aqueous	Fluorescence turn off	1×10^{-8} M	47
Perylene monoimide micelle	Aqueous	Fluorescence turn off	500 nM	48
Hydrophobically modified cationic cellulose micelles	Aqueous	Fluorescence turn off	0.5×10^{-7} M	49
Scutellarin–hispiduloside–glycerol (CIG)	Aqueous	Fluorescence turn off	9.1×10^{-8} M	50
Curcumin–glycerol (CG)	Aqueous	Fluorescence turn off	6.03×10^{-8} M	51
SAPAL-PY	Aqueous	Fluorescence turn off	1×10^{-12} M	This work

4. Conclusion

In summary, a water soluble probe incorporated with a pyrene chromophore was fabricated for the detection of a nitroaromatic explosive through fluorescence quenching. The sensor was selective towards picric acid (PA) over other tested analytes. Moreover, films have been successfully fabricated by simply immersing and drying into the probe solution. The detection limit was as low as 10^{-9} M for the film strips. Further, it can be recycled and reused for the selective detection of PA by a simple water wash. Hence, the fabricated probe could be a useful sensor with a high selectivity and sensitivity for the rapid detection of PA. Also, we anticipate that its biocompatibility could also be used for biological assays and bioimaging.

Conflicts of interest

There are no conflicts to declare.

References

1 S. Singh, *J. Hazard. Mater.*, 2007, **144**, 15–28.
2 B. W. Wang, K. Jiang, J. X. Li, S. H. Luo, Z. Y. Wang and H. F. Jiang, *Angew. Chem., Int. Ed.*, 2020, **59**, 2338–2343.
3 S. Shanmugaraju and P. S. Mukherjee, *Chem. Commun.*, 2015, **51**, 16014–16032.
4 Y. Zhao, L. Xu, F. Kong and L. Yu, *Chem. Eng. J.*, 2021, **416**, 129090.
5 R. M. Hebert and A. M. Jackovitz, in *Wildlife Toxicity Assessments for Chemicals of Military Concern*, Elsevier, 2015, pp. 271–277.
6 S. Dhiman, *et al.*, *Mater. Adv.*, 2021, **2**(20), 6466–6498.
7 X. Sun, Y. Wang and Y. Lei, *Chem. Soc. Rev.*, 2015, **44**, 8019–8061.
8 R. Shkumbatiuk, Y. R. Bazel, V. Andruch and M. Török, *Anal. Bioanal. Chem.*, 2005, **382**, 1431–1437.
9 C. Saridara, R. Brukh, Z. Iqbal and S. Mitra, *Anal. Chem.*, 2005, **77**, 1183–1187.
10 P. Sukhanov, A. Kushnir, E. Churilina, N. Maslova and G. Shatalov, *J. Anal. Chem.*, 2017, **72**, 468–472.
11 Y. Salinas, *et al.*, *Chem. Soc. Rev.*, 2012, **41**(3), 1261–1296.
12 L. Barron and E. Gilchrist, *Anal. Chim. Acta*, 2014, **806**, 27–54.
13 A. Hakonen, P. O. Andersson, M. S. Schmidt, T. Rindzevicius and M. Käll, *Anal. Chim. Acta*, 2015, **893**, 1–13.
14 T. Li, Q. Jia, L. Song, R. Su, Y. Lei, W. Zhou and H. Li, *Talanta*, 2009, **78**, 1497–1502.
15 A. Hilmi and J. H. Luong, *Anal. Chem.*, 2000, **72**, 4677–4682.
16 R. Luggar, M. Farquharson, J. Horrocks and R. Lacey, *X-Ray Spectrom.*, 1998, **27**, 87–94.
17 J. R. Junqueira, W. R. de Araujo, M. O. Salles and T. R. Paixão, *Talanta*, 2013, **104**, 162–168.
18 A. M. O'Mahony and J. Wang, *Anal. Methods*, 2013, **5**, 4296–4309.
19 Y. Salinas, R. Martínez-Máñez, M. D. Marcos, F. Sancenón, A. M. Costero, M. Parra and S. Gil, *Chem. Soc. Rev.*, 2012, **41**, 1261–1296.
20 A. Gowri, R. Vignesh and A. Kathiravan, *Spectrochim. Acta, Part A*, 2019, **220**, 117144.
21 M. Gupta and H.-I. Lee, *ACS Appl. Mater. Interfaces*, 2018, **10**, 41717–41723.
22 S. J. Toal and W. C. Trogler, *J. Mater. Chem.*, 2006, **16**, 2871–2883.
23 L. Lin, M. Rong, S. Lu, X. Song, Y. Zhong, J. Yan, Y. Wang and X. Chen, *Nanoscale*, 2015, **7**, 1872–1878.
24 A. H. Malik, S. Hussain, A. Kalita and P. K. Iyer, *ACS Appl. Mater. Interfaces*, 2015, **7**, 26968–26976.
25 W. Gong, H. Li, X. Gong, Z. Zhang and Z. Lu, *Spectrochim. Acta, Part A*, 2020, **233**, 118221.
26 J. D. Desai and I. M. Banat, *Microbiol. Mol. Biol. Rev.*, 1997, **61**, 47–64.
27 Z. I. Rajput, S.-H. Hu, C.-W. Xiao and A. G. Arijo, *J. Zhejiang Univ., Sci., B*, 2007, **8**, 153–161.
28 G. Francis, Z. Kerem, H. P. Makkar and K. Becker, *Br. J. Nutr.*, 2002, **88**, 587–605.
29 D. Kregiel, J. Berlowska, I. Witonska, H. Antolak, C. Proestos, M. Babic, L. Babic and B. Zhang, *Appl. Charact. Surfactants*, 2017, **6**, 184–205.
30 S. Karuppannan and J. C. Chambron, *Chem. – Asian J.*, 2011, **6**, 964–984.
31 X. Liu, L. Wang, X. Song, H. Song, J. R. Zhao and S. Wang, *Carbohydr. Polym.*, 2012, **90**, 218–223.
32 J. Sirvio, U. Hyvakko, H. Liimatainen, J. Niinimaki and O. Hormi, *Carbohydr. Polym.*, 2011, **83**, 1293–1297.
33 G. Dinda, D. Halder, A. Mitra, N. Pal, C. Vázquez-Vázquez and M. A. López-Quintela, *New J. Chem.*, 2017, **41**, 10703–10711.
34 W. Smułek, A. Zdarta, M. Łuczak, P. Krawczyk, T. Jesionowski and E. Kaczorek, *Colloids Surf., B*, 2016, **142**, 207–213.
35 L. Yu, X. Tang, L. Chen, M. Wang, J. Jian, S. Cao, X. Wang, N. Kang and F. Qiu, *Fitoterapia*, 2012, **83**, 1636–1642.
36 H. Amer, T. Nypelö, I. Sulaeva, M. Bacher, U. Henniges, A. Potthast and T. Rosenau, *Biomacromolecules*, 2016, **17**, 2972–2980.
37 P. Eaton, P. Quaresma, C. Soares, C. Neves, M. De Almeida, E. Pereira and P. West, *Ultramicroscopy*, 2017, **182**, 179–190.
38 S. Bhattacharjee, *J. Controlled Release*, 2016, **235**, 337–351.
39 M. Behera and G. Giri, *Mater. Sci.-Pol.*, 2014, **32**, 702–708.
40 I. Charhouf, A. Bennamara, A. Abourriche, A. Chenite, J. Zhu and M. Berrada, *Biosensors*, 2014, **16**, 18.
41 O. G. Idemudia, A. P. Sadimenko, A. J. Afolayan and E. C. Hosten, *Bioinorg. Chem. Appl.*, 2015, **2015**, 717089.
42 S. Hirano, T. Fukuda and M. Sato, *Agric. Biol. Chem.*, 1974, **38**, 2539–2543.
43 M. Dolaz, V. McKee, A. Golcu and M. Tumer, *Curr. Org. Chem.*, 2010, **14**, 281–288.
44 S. Dhiman, *et al.*, *Mater. Adv.*, 2021, **2**(20), 6466–6498.
45 S. Zhang, L. Ding, F. Lü, T. Liu and Y. Fang, *Spectrochim. Acta, Part A*, 2012, **97**, 31–37.

46 S. Koev, P. Dykstra, X. Luo, G. Rubloff, W. Bentley, G. Payne and R. Ghodssi, *Lab Chip*, 2010, **10**, 3026–3042.
47 H. Du, G. He, T. Liu, L. Ding and Y. Fang, *J. Photochem. Photobiol., A*, 2011, **217**, 356–362.
48 W. Li, H. Zhou, M. A. H. Nawaz, N. Niu, N. Yang, J. Ren and C. Yu, *Anal. Methods*, 2020, **12**, 5353–5359.
49 L. Zhang, C. Zhao, J. Zhou and T. Kondo, *J. Mater. Chem. C*, 2013, **1**, 5756–5764.
50 S. Chakravarty, B. Gogoi and N. S. Sarma, *J. Lumin.*, 2015, **165**, 6–14.
51 M. Y. Khorasani, H. Langari, S. B. T. Sany, M. Rezayi and A. Sahebkar, *Mater. Sci. Eng., C*, 2019, **103**, 109792.